COHERENT INFRARED RADIATION FROM THE ALS GENERATED VIA FEMTOSECOND LASER MODULATION OF THE ELECTRON BEAM*

J.M. Byrd, Z. Hao, M.C. Martin, D.S. Robin, F. Sannibale, R.W. Schoenlein, M. Venturini, A.A. Zholents, M.S. Zolotorev, Lawrence Berkeley National Laboratory, Berkeley, CA 94720, USA

Abstract

Interaction of an electron beam with a femtosecond laser pulse co-propagating through a wiggler at the ALS produces large modulation of the electron energies within a short ~100 fs slice of the electron bunch. Propagating around the storage ring, this bunch develops a longitudinal density perturbation due to the dispersion of electron trajectories. The length of the perturbation evolves with a distance from the wiggler but is much shorter than the electron bunch length. This perturbation causes the electron bunch to emit short pulses of temporally and spatially coherent infrared light which are automatically synchronized to the modulating laser. The intensity and spectra of the infrared light were measured in two storage ring locations for a nominal ALS lattice and for an experimental lattice with the higher momentum compaction factor. The onset of instability stimulated by laser e-beam interaction had been discovered. The infrared signal is now routinely used as a sensitive monitor for a fine tuning of the laser beam alignment during data accumulation in the experiments with femtosecond x-ray pulses.

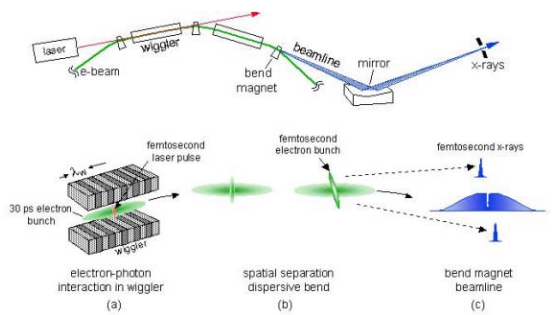

Figure 1. A schematic of the laser - electron beam interaction producing fs x-ray pulses.

INTRODUCTION

The source of femtosecond (fs) x-ray pulses has been in operation at the Advanced Light Source in the Berkeley Lab [1]. A detailed description of this source can be found elsewhere [2-4]. We recall that this source is based on laser interaction with relativistic electron beam in a wiggler magnet as schematically illustrated in Fig 1. A 100-fs optical pulse of moderate energy modulates the energy of an ultra- short (~ 30 micron) slice of a stored electron bunch as they co-propagate through a wiggler in a storage ring (Fig.1a). The energy-modulated electron slice is spatially separated from the main bunch in a dispersive section of the storage ring (Fig.1b) and used to radiate fs x-rays at a bend-magnet or insertion-device (Fig.1c). It was also noted [4] that energy modulation of electrons creates a small perturbation to the electron bunch longitudinal density consisting of a dip and two side bumps. This perturbation is due to the dispersion of the electron trajectories, which causes the high and low energy electrons to move far away from their original positions while the electron bunch moves from the wiggler to the radiation source. This perturbation gives rise to an electron emission of a temporally and spatially coherent infrared light. The intensity of this radiation is proportional to a square of the number of displaced electrons. Here we report measurements of this signal and related phenomena.

*This work was supported by Office of Science, U.S. Dept. of Energy, under Contract No. DE-AC03-76SF00098.

CHARACTERIZATION OF THE INFRARED PULSE

At the middle of the wiggler, the initial Gaussian electron distribution in the absence of the laser pulse is described by: $P_o(x_o,x_o',E_o,t_o) \sim \exp\left[-0.5\left(x_o^2+x_o'^2+E_o^2\right)-0.5t_o^2/\sigma_{t-e}^2\right]$, where x_o, x_o', E_o are the electron horizontal coordinate and angle, and the electron relative energy deviation normalized to their respective rms values (σ_x, $\sigma_{x'}$, and σ_E), ct_o is the electron longitudinal position with respect to the bunch center, c is the speed of light and $\sigma_{t\text{-}e}$ is the rms electron bunch duration. Energy modulation of the electrons co-propagating with the laser pulse through the wiggler is described by: $\Delta E = A_E \mathrm{Cos}(\omega_L t_0)\mathrm{e}^{-t_0^2/4\sigma_{t-L}^2}$, where A_E is the peak amplitude of the energy modulation, ω_L is the laser frequency and $\sigma_{t\text{-}L}$ is the rms width of the laser pulse. Thus the electron energy after the wiggler is $E_1 = E_o + \Delta E$. Following interaction with a fs optical pulse in the wiggler, the temporal distribution of electrons within the bunch is determined by the energy modulation and the time-of-flight characteristics of the storage ring lattice R_{51}, R_{52}, R_{56} [5]. The temporal distribution of electrons at the radiating source is given by: $P_R(t_R) = \iiint dE_1 dx_0 dx_0' P_o(x_0, x_0', E_1, t_R)$, where

$t_R - t_o = (R_{56}E1 + x_o\sigma_x R_{51} + x_o'\sigma_x R_{52})c^{-1}$ accounts for the particle path length differences (time shifts) during the electron beam path from the wiggler center to the radiation source due to the electron coordinate, angle and energy off-set.

Measurements of the infrared radiation at the ALS were performed at two bend magnet sources located: (i) one-half sector downstream from the wiggler at beamline 5.3.1 (BL5.3.1), and (ii) 8.5 sectors downstream from the wiggler at beamline 1.4 (BL1.4). Measurements were carried out with a nominal 1.5GeV lattice (NL) and with an experimental 1.5GeV lattice (EL) where the momentum compaction factor and the electron beam emittance were practically doubled. The time-of-flight parameters from the wiggler magnet to the BL5.3.1 for the NL (and EL) are R_{51} =-0.013 (-0.049), R_{52} =0.27 (0.23)m, and R_{56} =0.013 (0.017) m, and from the wiggler magnet to the BL4.1 are R_{51} =0.014 (0.051), R_{52} =0.18 (0.23) m, and R_{56} =0.20 (0.40) m. The three quadrupole families of the triple bend achromat cells of the ALS were tuned in order to produce the large momentum compaction factor while keeping the betatron tunes constant. Fig.2a and Fig.2c show a calculated electron longitudinal distribution in two source locations and for the two lattices assuming an energy modulation of A_E =6 and $\sigma_{t\text{-}L}$ =45 fs. In all cases, electrons with ΔE<0 accumulate toward the head of the bunch while electrons with ΔE>0 accumulate toward the tail of the bunch, creating a dip in the center of the temporal distribution and two side bumps (at earlier and later times). The uncorrelated energy spread of electrons causes a smearing of the distributions which grows with increasing distance from the wiggler. A corresponding spectrum of the infrared signal for all four cases is shown in Fig. 2b and Fig. 2d.

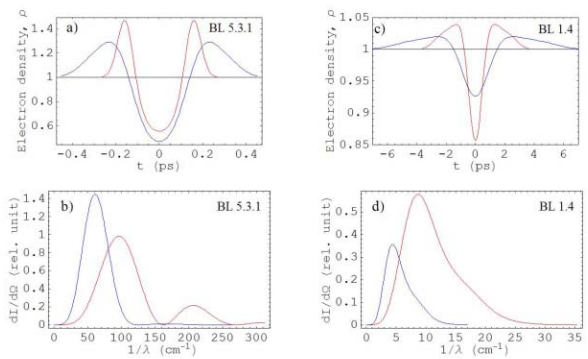

Figure 2: The predicted perturbation in the electron density distribution and the spectrum of the infrared radiation caused by this perturbation shown for BL5.3.1 and BL1.4 for the nominal lattice (red line) and for the experimental lattice with an increased momentum compaction factor (blue line). Plots a) and c) show the distribution and plots b) and d) show the corresponding spectrum.

MEASUREMENTS

A schematic of measurement apparatus is shown in Fig. 3. The infrared radiation is directed by two metallic mirrors into the FTIR spectrometer (IFS 66V, *Bruker*). The signal is then detected by a bolometer (liquid He cooled, HD3, *Infrared Laboratories Inc*.) equipped with a filter which cuts out the background radiation with spectral components above ν = 90 cm^{-1}, where ν is the wave number. The bolometer response has a relatively fast rise time and a long ~ 0.7 ms fall time defined by its cooling

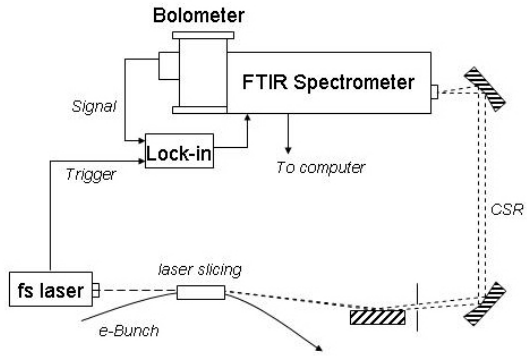

Figure 3: A schematic of the measurement apparatus.

time. A digital oscilloscope and the phase sensitive lock-in amplifier (SR844, *SRS*) are used for data acquisition.

Fig. 4 shows the oscilloscope trace of the infrared signal measured at BL1.4 for the electron bunch current of ~1 mA. This current is much below a threshold of the bursting instability observed previously [6]. The oscilloscope was set in the averaging mode and was

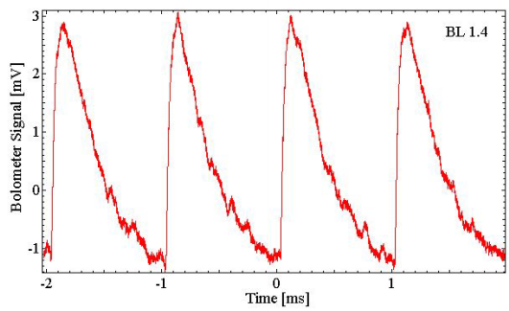

Figure 4: The infrared signal measured with the nominal lattice at BL1.4 with laser turned on and electron bunch current of ~1 mA.

triggered by the signal derived from the modulating laser operating at approximately 1 kHz repetition rate. The waveform clearly exhibits the periodicity of 1 ms corresponding to the repetition rate of the modulating laser. Zero signal was observed when the laser was blocked from entering the wiggler magnet, indicating the dominance of the coherent radiation by the laser induced electron density perturbation over the spontaneous emission of the entire electron bunch. The shape of the oscilloscope signal is completely determined by the bolometer's response. The signal amplitude assumes positive and negative values due to the detector's AC-coupling to the oscilloscope. With the nominal lattice, the amplitude of the signal, measured as a peak-to-peak value on the oscilloscope, followed a quadratic dependence from the electron bunch current even when the current was above the threshold of the bursting instability. However, a similar measurement with the experimental

lattice revealed a dramatic change showing a much stronger dependence (see, Fig.5). We explain it by the onset of the stimulated and self amplified instability, *i.e.* instability caused by initial electron density perturbation

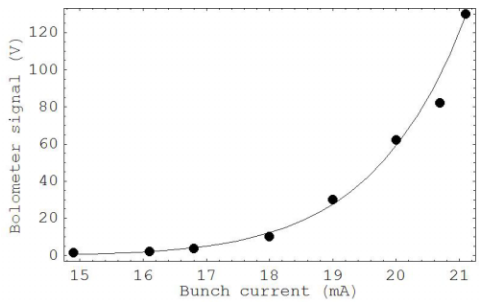

Figure 5: The infrared signal measured with the experimental lattice at BL1.4 as the function of the electron bunch current. For all data points the electron bunch current exceeds the threshold of bursting instability.

followed by self amplification via coherent synchrotron radiation (CSR). This effect is similar to the instability previously considered in [7,8] and measured in [6,9]. In a qualitative agreement with [7], the data points in Fig.5 are fit by the function $u(I) = u(16\,\mathrm{mA})\,\mathrm{Exp}\left\{b\sqrt{I - I_{th}}\right\}$ with the threshold current I_{th} =12 mA and a coefficient b =4.2. We also noticed large fluctuations in the signal that could possibly be explained by the destructive interference between the laser stimulated radiation and self amplified spontaneous emission (bursting) occurring above the instability threshold.

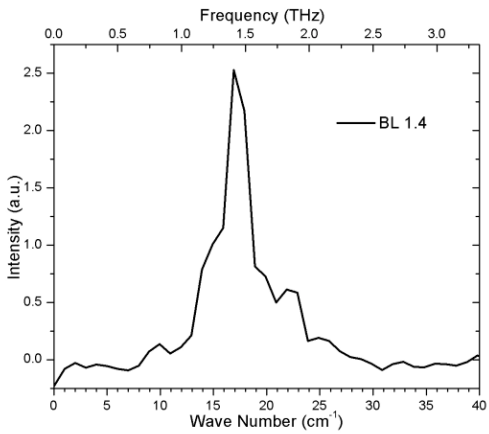

Figure 6: The spectral measurement of the infrared signal at BL1.4.

We note that since first measurements of the infrared signal in November 2003, the bolometer signal is routinely used as a sensitive monitor for a fine tuning of the laser beam alignment during data accumulation in the experiments with femtosecond x-ray pulses.

The ALS vacuum chamber effectively cuts the radiation spectra with $\nu < 20$ cm^{-1} at BL5.3.1 and at $\nu < 5$ cm^{-1} at BL1.4 while bolometer's sensitivity rapidly rolls down for $\nu < 15$ cm^{-1}. Thus, the spectral measurement on BL 1.4 in Fig. 6 shows only the observable part of the calculated spectra. Spectral measurements were also made at BL5.3.1, and roughly agree with the predicted spectra shown in Fig. 2b. However, quantitative interpretation of these measurements is somewhat ambiguous and model dependent. This is due to waveguide effects as the signal propagates through the narrow gap vacuum chamber and exits through a small diameter diamond window. Simulations of these effects using the SRW code [10] indicate that this waveguide creates a wavelength dependent spatial modulation of the radiation intensity at the exit window which is sensitive to the practical details of the waveguide geometry. In the near future we plan to replace the present window with a window with a larger diameter, and repeat the spectral measurements.

REFERENCES

[1] R.W. Schoenlein, et *al*., *Science*, Mar 24, (2000) 2237.
[2] A. Zholents, M. Zolotorev, *Phys. Rev. Lett*. **76**, 912, (1996).
[3] R.W. Schoenlein, et *al*., Comptes Rendus de l'Academie des Sciences, Serie IV, Paris, vol.2, (no.10), Editions Elsevier, Dec. 2001. p.1373-88.
[4] R.W. Schoenlein, et *al*., Appl. Phys. B, 1-10, 2000.
[5] K.L. Brown et *al*., CERN 80-04, (1980).
[6] J. M. Byrd et al., *Phys. Rev. Lett.* **89**, 224801 (2002).
[7] G. Stupakov and S. Heifets, *Phys. Rev. ST* **5**, 054402 (2002).
[8] M. Venturini and R. Warnock, *Phys. Rev. Lett.* **89**, 224802 (2002).
[9] M.Abo-Bakr *et al., Part. Acc. Conf. PAC03*, Portland, OR USA, May 12-16, 2003.
[10] O. Chubar and P.Ellaume, Synchrotron Radiation Workshop (SRW) code, http://www.esrf.fr/machine/groups/insertion_devices/Codes/software.html